

Fermi National Accelerator Laboratory

FERMILAB-Pub-87/232-A
December 1987

COMPOSITE LEPTOQUARKS IN HADRONIC COLLIDERS

Oscar J. P. Éboli[†]

*Center for Theoretical Physics
Laboratory for Nuclear Science
and Department of Physics
Massachusetts Institute of Technology
Cambridge, Massachusetts 02139 U.S.A.*

and

Angela V. Olinto

*NASA/Fermilab Astrophysics Center
Fermi National Accelerator Laboratory
Box 500, Batavia, IL 60510*

Submitted to: *Physical Review D*

[†] Address after March 1, 1988: Instituto da Física de Universidade de São Paulo, C.P. 20516, CEP 01498, São Paulo, BRAZIL



ABSTRACT

We study the production of composite scalar leptoquarks in hadronic colliders (CERN $\bar{p}p$, TEVATRON $\bar{p}p$ and SSC pp). We examine its direct single production via $qg \rightarrow l + \text{leptoquark}$, and its effect on the production of lepton pairs ($\bar{p} p \rightarrow \ell^+ \ell^-$).

INTRODUCTION

The standard electroweak theory provides a very satisfactory description of the elementary particle phenomena up to the presently available energies. However, the proliferation of fermion generations, the complex pattern of their masses and mixing angles, and the unnaturalness of the Higgs sector make substructure models somewhat appealing. Composite models exhibit a very rich spectrum which includes many new states such as excitations of the known particles (leptons, quarks and vector bosons) and bound states which cannot be viewed as excitations of the familiar particles since they carry rather unusual quantum numbers. Among these, there are leptoquarks which are particles carrying lepton and baryon number. Leptoquarks are also present in a variety of theories beyond the standard model such as some technicolor schemes¹ and grand unified theories.² In the present work we study the production of scalar leptoquarks in the context of the Abbott-Farhi model.³

The Lagrangian of the Abbott-Farhi model has the same form as the standard model one with the usual field assignments. However, the parameters determining the potential for the scalar field and the strength of the $SU(2)_L$ gauge interaction, are such that no spontaneous symmetry breaking occurs and the $SU(2)_L$ gauge interaction is confining. This model is essentially the confining version of the standard model and is called the strongly coupled standard model (SCSM). Weakly interacting physical particles, such as left-handed fermions and intermediate vector bosons, are composite $SU(2)_L$ singlets due to the strong $SU(2)_L$ force. For instance, the physical left-handed fermions are bound states of a preonic scalar and a preonic dynamical left-handed fermion. Provided some

dynamical assumptions on the model hold true, it has been shown⁴ that the predictions of the SCSM model are consistent with the present experimental data.

We denote the preonic left-handed fermions by ψ_L^a , with the flavor index a running from 1 to 12 for three families. ψ_L^a belongs to a $\underline{2}$ representation of the $SU(2)_L$ and to the $(0, 1/2)$ representation of the Lorentz group. The scalar leptoquarks in the SCSM model are bound states of the form $\psi_L^a \psi_L^b$ where ψ_L^a carries baryon number while ψ_L^b carries lepton number. We define S^{ab} as the interpolating field for the scalar leptoquarks. S^{ab} is anti-symmetric in its flavor indices due to Fermi–Dirac statistics. The electric charge of S^{ab} is $-1/3$ and it belongs to the $\underline{3}$ representation of $SU(3)_{\text{color}}$

Since the SCSM model cannot be analyzed perturbatively at the energy scale of interest, we describe the interaction between leptoquarks and physical left-handed fermions by an effective Lagrangian. We assume that the low energy interactions of S^{ab} are described by

$$\mathcal{L}_{\text{int}} = \frac{\lambda_{ab}}{2} \left(S_{ab}^\dagger L^{aT} C \tau^2 L^b + \text{h.c.} \right) \quad (1.1)$$

where L^a stands for physical left-handed doublets under the global $SU(2)$ symmetry of the model.⁵ C is the charge conjugation matrix and τ^i are the Pauli matrices. The above \mathcal{L}_{int} conserves baryon and lepton number, charge, and color.

The absence of experimental evidence for compositeness constrains the low energy phenomenology of the SCSM. These constraints can, in principle, place bounds on the leptoquark mass (M_{LQ}) and coupling constant (λ_{ab}). In practice, contributions from other states soften these bounds,⁶ so that M_{LQ} and λ_{ab} can be considered free parameters. However, an educated guess for the coupling λ_{ab} can be made as follows. Since the Z and the W 's are bound states of two preonic fields in the SCSM, it is natural to assume

that the coupling of leptoquarks to physical left-handed fields is of the same order of the coupling of these fermions to W 's and Z . Therefore, we expect λ_{ab} to be of order 1.

Experimental searches for leptoquarks in e^+e^- colliders⁷ have established a lower limit on M_{LQ} of 23 GeV, while the searches in $\bar{p}p$ colliders⁸ yield a lower limit of 33 GeV (for leptoquark decaying into jet + (μ or ν)).

In §II we analyze the production of single leptoquarks in hadronic colliders. We study indirect evidence for leptoquarks in §III, and in §IV we conclude.

II. PRODUCTION OF SINGLE LEPTOQUARKS

The production of a single leptoquark in hadronic colliders must be associated with that of a lepton since baryon and lepton numbers are conserved by the effective Lagrangian (1.1). This occurs via the subprocess

$$\text{quark} + \text{gluon} \longrightarrow \text{leptoquark} + \text{lepton}$$

whose relevant Feynman diagrams are shown in Fig. 1. The elementary cross section for this subprocess is, neglecting lepton and quark masses,

$$\frac{d\hat{\sigma}_{\text{single}}}{d\hat{t}} = \frac{\lambda_{ab}^2 \alpha_s}{24\hat{s}^2} \left[-\frac{\hat{t}}{8\hat{s}} - \frac{1}{4} \frac{\hat{t}\hat{u}^2}{\hat{s}(\hat{u} - M_{LQ}^2)^2} + \frac{\hat{u}\hat{t}}{4\hat{s}(\hat{u} - M_{LQ}^2)} \right], \quad (2.1)$$

where $\hat{t} = -\frac{\hat{s}}{2}(1 - \cos\theta)$, and θ is the scattering angle between the quark and the leptoquark in the C.M. frame of the subprocess.

In order to evaluate the cross section for the process pp (or $\bar{p}p$) \rightarrow leptoquark + anything, we must fold (2.1) with the appropriate structure functions, *i.e.*,

$$\begin{aligned} \sigma_{\text{single}}(\overset{(-)}{s} \text{ X}) &= \int_{-y_0}^{y_0} dy \int_{M_{LQ}^2/s}^{e^{-2|y|}} d\tau \left[F(\sqrt{\tau} e^y; Q^2) G(\sqrt{\tau} e^{-y}; Q^2) \right. \\ &\quad \left. + G(\sqrt{\tau} e^y; Q^2) F(\sqrt{\tau} e^{-y}; Q^2) \right] \\ &\quad \times \int_{-x_0}^{x_0} dz \frac{d\hat{\sigma}_{\text{single}}}{dz}, \end{aligned} \quad (2.2a)$$

where y_c is the cut in rapidity,

$$\frac{d\hat{\sigma}_{\text{single}}}{dz} = \frac{\beta\hat{s}}{2} \frac{d\hat{\sigma}_{\text{single}}}{d\hat{t}}, \quad (2.2b)$$

$$\beta = 1 - \frac{M_{\text{LQ}}^2}{\hat{s}}, \text{ and} \quad (2.2c)$$

$$z_0 = \text{Min} \left\{ \frac{\beta}{1 + M_{\text{LQ}}^2/\hat{s}} \tanh(y_c - y); 1 \right\}. \quad (2.2d)$$

The factor F in (2.2) is $2u_s + u_v + 2c_s$ for $\mathbf{X} = \ell^\pm$, and $2d_s + d_v + 2s_s$ for $\mathbf{X} = \bar{\nu}_e$.

Setting the couplings λ_{ab} equal to λ , we obtain

$$\int_{-z_0}^{z_0} dz \frac{d\hat{\sigma}_{\text{single}}}{dz} = \frac{\alpha_s \lambda^2}{96\hat{s}} \left\{ \frac{z_0}{4} (1 - \eta)^2 + \eta(1 + \eta) \ln \left[\frac{(1 - z_0) + \eta(1 + z_0)}{(1 + z_0) + \eta(1 - z_0)} \right] + \eta(1 - \eta)z_0 + \frac{\eta^2(1 - \eta)z_0}{\eta + \frac{1}{4}(1 - \eta)^2(1 - z_0^2)} \right\} \quad (2.2e)$$

where $\eta = M_{\text{LQ}}^2/\hat{s}$.

In the numerical calculations, we have evaluated the strong coupling α_s at \hat{s} and we have used the Duke–Owens I structure functions.⁹ Imposing a rapidity $|y_c| < 2.5$, and taking λ to be 0.6, 1.2, and 1.8, we evaluated σ_{single} for the CERN ($\sqrt{s} = 630\text{MeV}$), the TEVATRON ($\sqrt{s} = 2\text{TeV}$), and the SSC ($\sqrt{s} = 40\text{TeV}$). Our results are summarized in Figs. 2–4. We have verified that the use of another rapidity cut ($|y_c| < 1.5$) does not alter sensibly the above results.

Since a leptoquark can decay into a pair ℓq or $\nu q'$, the characteristic signals for the single leptoquark production are

$$(a) \text{ jet} + \nu_\ell + \bar{\nu}_\ell, \quad ,$$

$$(b) \text{ jet} + \ell^\pm + \bar{\nu}_\ell, \quad ,$$

or

(c) jet + ℓ^+ + ℓ^- .

Signal (a) corresponds to a monojet final state. Although this signal is quite striking it will be overwhelmed by standard model processes such as $\bar{p} p \rightarrow Z(\rightarrow \nu\bar{\nu}) + g$ (or q), which are expected¹⁰ to have a much larger cross section than the single leptoquark production. The same is true for signal (b) since standard model subprocesses¹⁰, like the production of $W(\rightarrow \ell^\pm \bar{\nu}) + g$ (or q), yield the same signal with larger cross sections. Introducing cuts may help distinguish signals (a) and (b) from the background.

Signal (c) provides the cleanest signature for the existence of leptoquarks. Standard model backgrounds, like $\bar{p} p \rightarrow Z(\rightarrow \ell^+\ell^-) + q$ (or g), can be eliminated by discarding events in which the invariant mass of the lepton pair is close to the Z mass. The possibility of QCD events faking this signal deserves further study. (A careful Monte Carlo analyses of the background is needed.)

In order to establish the existence of leptoquarks we require the occurrence of 500 events/year yielding $\ell^+ + \ell^- + \text{jet}$. Since the couplings $Sq\ell$ and $Sq'\nu$ are expected to be approximately equal we take $\sigma(\ell^+ + \ell^- + \text{jet}) = \sigma(S + \ell^\pm)/2$. From Figs. 2 - 4 we can infer that for λ equal to 0.6 (1.8) the maximum M_{LQ} observable is 35 (50) GeV, 60 (90) GeV, and 1.3 (2.0) TeV for the CERN, TEVATRON and SSC colliders, assuming integrated luminosities of 10^{37} , 10^{37} , and 10^{40} cm^2/year .

III. INDIRECT EVIDENCE FOR LEPTOQUARKS

The existence of composite leptoquarks can also be investigated through their effects in the dilepton production ($\bar{p} p \rightarrow \ell^+\ell^-$). Since they couple to both leptons and quarks,

there is a new channel to this process in addition to the usual $q \bar{q} \rightarrow \gamma, Z \rightarrow \ell^+ \ell^-$. The relevant Feynman diagrams are shown in Fig. 5. The elementary cross section is given by

$$\begin{aligned}
\frac{d\hat{\sigma}}{d\hat{t}} = & \frac{1}{16\pi\hat{s}^2} \left\{ \frac{32\pi^2\alpha_{em}^2q^2}{\hat{s}^2} [\hat{t}^2 + \hat{u}^2] \right. \\
& + \frac{8\pi^2\alpha_{em}^2}{\sin^4\theta_W \cos^4\theta_W} \frac{1}{(\hat{s} - M_Z^2)^2} \left[\frac{1}{4} (C_V^{q^2} + C_A^{q^2}) (C_V^{\ell^2} + C_A^{\ell^2}) \right. \\
& \times (\hat{t}^2 + \hat{u}^2) + C_A^q C_V^q C_A^\ell C_V^\ell (\hat{u}^2 - \hat{t}^2) \left. \right] \\
& + \frac{16\pi^2\alpha_{em}^2}{\sin^2\theta_W \cos^2\theta_W} \frac{1}{\hat{s}(\hat{s} - M_Z^2)} \left[C_V^q C_V^\ell (\hat{u}^2 + \hat{t}^2) + C_A^q C_A^\ell (\hat{u}^2 - \hat{t}^2) \right] \\
& + \frac{\lambda^4}{64} \frac{\hat{u}^2}{(\hat{u} - M_{LQ}^2)^2} - \pi\lambda^2\alpha_{em}q \frac{\hat{\mu}^2}{\hat{s}(\hat{\mu} - M_{LQ}^2)} \\
& - \frac{\pi\lambda^2\alpha_{em}}{4\sin^2\theta_W \cos^2\theta_W} (C_V^q - C_A^q) (C_V^\ell - C_A^\ell) \frac{\hat{u}^2}{(\hat{s} - M_Z^2)(\hat{u} - M_{LQ}^2)},
\end{aligned} \tag{3.1}$$

where M_Z is the mass of the Z boson, θ_W is the weak mixing angle, the charge of the quark is $-qe$, and, with our conventions,

$$C_V = I_x + 2q \sin^2 \theta_W$$

$$C_A = I_x .$$

The distribution in invariant mass of the pair can be obtained through

$$\begin{aligned}
\frac{d\sigma}{dM} = & \frac{2M}{s} \sum_{ij} \int_{-y^*}^{y^*} \left\{ q_i (\sqrt{\tau} e^y) q_j (\sqrt{\tau} e^{-y}) \right. \\
& \left. + q_i (\sqrt{\tau} e^{-y}) q_j (\sqrt{\tau} e^y) \right\} \int_{-x_0}^{x_0} dz \frac{d\hat{\sigma}}{dz}
\end{aligned} \tag{3.2}$$

where the above summation is over the relevant quark species, $M^2 = \hat{s}$, $\tau = \hat{s}/s$ and

$$y^* = \text{Min} \left\{ y_c, \ln \frac{1}{\sqrt{\tau}} \right\} .$$

The results for CERN, TEVATRON and SSC are shown in Figs. 6 – 8. [We considered only one kind of final lepton when obtaining Figs. 6 – 8.] From these we can see that the

$\frac{d\sigma}{dm}$ distribution is sensibly modified at large M provided that the coupling (λ) is larger than 1.

In order to verify the possibility of observing this signal we computed the ratio $\sigma(\lambda \neq 0)/\sigma(\lambda = 0)$, where σ is the cross section for producing dileptons with P_T larger than a given value P_{T_0} . From Figs. 6 - 8 we see that the higher the cut P_{T_0} , the easier it is to search for deviations from the standard model ($\lambda = 0$). Taking P_{T_0} to be 60 GeV, 75 GeV, and 500 GeV for the CERN, TEVATRON, and SSC, respectively, we obtain Figs. 9 - 11. Requiring this ratio to be approximately 2 in order to establish the existence of leptoquarks, we should be able to look for leptoquarks with masses up to 130 GeV, 150 GeV and 1.3 TeV at CERN, TEVATRON, and SSC, (taking $\lambda = 1.8$).

IV. CONCLUSION

We have studied two effects of leptoquarks on the outcome of hadronic colliders. The direct single production of a leptoquark can be best observed as a jet plus a lepton pair in the final state, where the invariant mass of the pair differs from the Z mass. This kind of process can be observed at the CERN, TEVATRON, and SSC colliders for leptoquark masses up to 50 GeV, 90 GeV, and 2 TeV.

An indirect evidence for the existence of leptoquarks can be seen due to the additional channel for $\bar{p} p \rightarrow \ell^+ \ell^-$. This reaction enables the CERN, TEVATRON, and SSC colliders to probe leptoquark masses up to 130 GeV, 150 GeV, and 1.3 TeV.

ACKNOWLEDGEMENTS

This work was supported in part by funds provided by the U. S. Department of Energy under contract #DE-AC02-76ER03069, by Conselho Nacional de Desenvolvimento Científico e Tecnológico (CNPq), Brazil, and by D.O.E. and NASA at Fermilab.

REFERENCES

1. S. Dimopoulos, *Nucl. Phys.* **B168**, 69 (1980); E. Farhi and L. Susskind, *Phys. Rev.* **D20**, 3404 (1979).
2. See, *e.g.*, P. Langacher, *Phys. Rev.* **72**, 185 (1981).
3. L. Abbott and E. Farhi, *Phys. Lett.* **101B**, 69 (1981); *Nucl. Phys.* **B189**, 547 (1981).
4. M. Claudson, E. Farhi and R. Jaffe, *Phys. Rev.* **D34**, 873 (1986).
5. J. Wudka, *Phys. Lett.* **167B**, 337 (1986).
6. C. Korpa and Z. Ryzak, *Phys. Rev.* **D34**, 2139 (1986).
7. M. Davies, in *Proceedings of the XXIII International Conference on High Energy Physics*, Berkeley, CA, 1986, S. C. Loken, ed. (World Scientific, Singapore, 1987), p. 25.
8. UAI collaboration, as reported by S. Geer, in *EPS Conference on High Energy Physics*, Uppsala (1987).
9. D. Duke and J. Owens, *Phys. Rev.* **D30**, 49 (1984).
10. E. Eichten, I. Hinchliffe, K. Lane and C. Quigg, *Rev. Mod. Phys.* **56**, 579 (1984).

FIGURE CAPTIONS

Fig. 1: Feynman diagrams for the subprocess $q + g \rightarrow \ell + \text{leptoquark}$.

Fig. 2: Cross section for the production of pairs: (a) $\ell^\pm + \text{leptoquark}$; (b) $\bar{\nu} + \text{leptoquark}$ at the CERN collider. Solid, dashed, and dotted lines correspond to $\lambda = 0.6, 1.2,$ and 1.8 .

Fig. 3: Same as Fig. 2 for the TEVATRON.

Fig. 4: Same as Fig. 2 for the SSC.

Fig. 5: Feynman diagrams for the subprocess $q + \bar{q} \rightarrow \ell^+ + \ell^-$.

Fig. 6: $\frac{d\sigma}{dM}$ for dilepton production at the CERN: (a) $M_{LQ} = 50$ GeV; (b) $M_{LQ} = 100$ GeV. The solid, dashed, and dot-dashed lines correspond to $\lambda = 0, 0.6,$ and $1.8,$ respectively.

Fig. 7: $\frac{d\sigma}{dM}$ for dilepton production at the TEVATRON (a) $M_{LQ} = 50$ GeV; (b) $M_{LQ} = 150$ GeV. Same convention as in Fig. 6.

Fig. 8 $\frac{d\sigma}{dM}$ for dilepton production at the SSC (a) $M_{LQ} = 100$ GeV; (b) $M_{LQ} = 700$ GeV. Same convention as in Fig. 6.

Fig. 9: $\sigma(\lambda \neq 0)/\sigma(\lambda = 0)$ for CERN. The solid and dashed lines correspond to $\lambda = 0.6$ and 1.8 .

Fig. 10: Same as Fig. 9 for the TEVATRON.

Fig. 11: Same as Fig. 9 for the SSC.

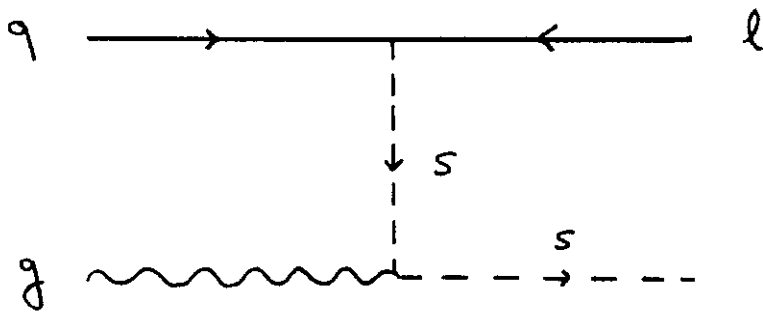
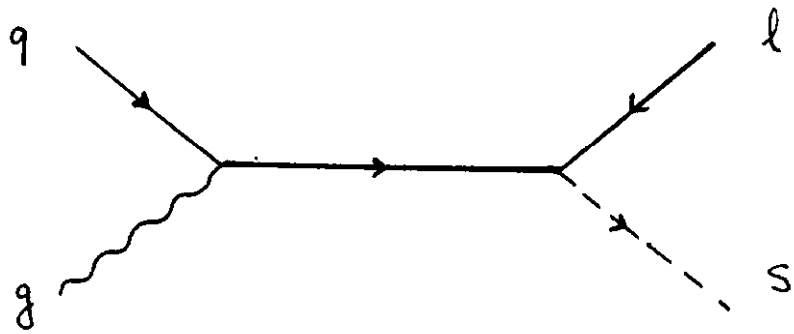


Fig. 1

Figure 2a

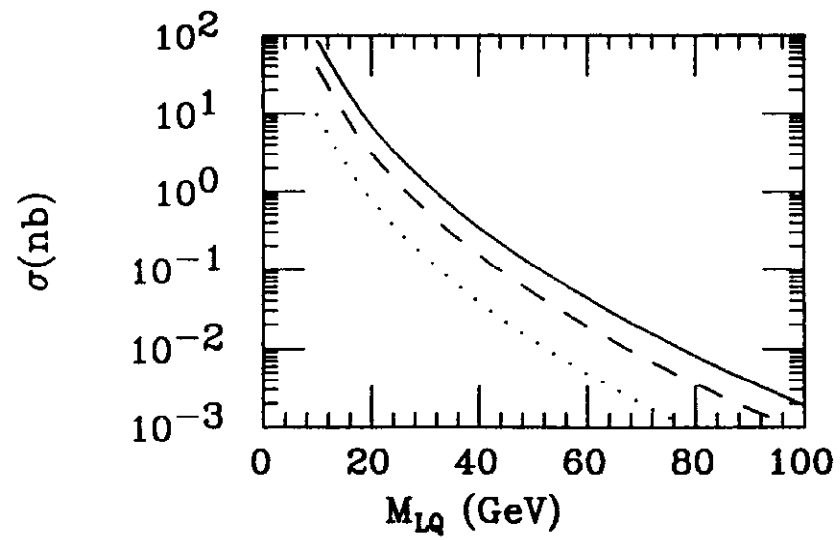


Figure 2b

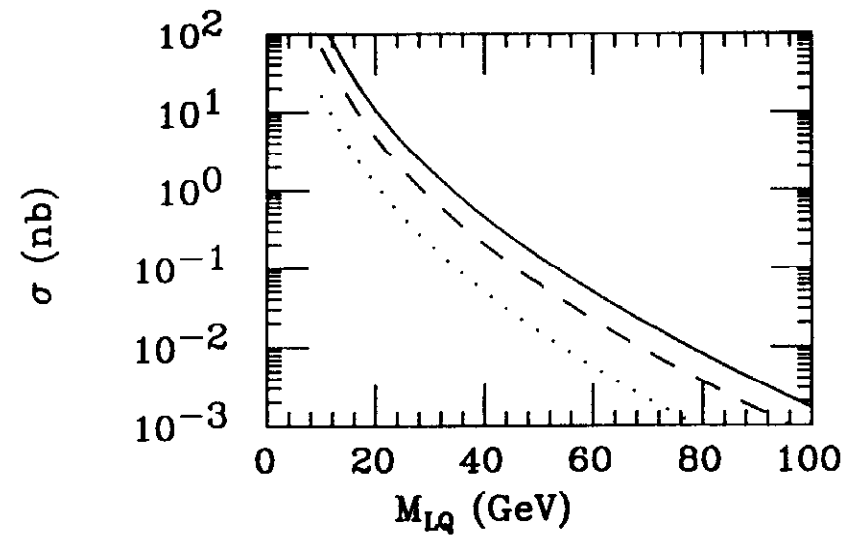


Figure 3a

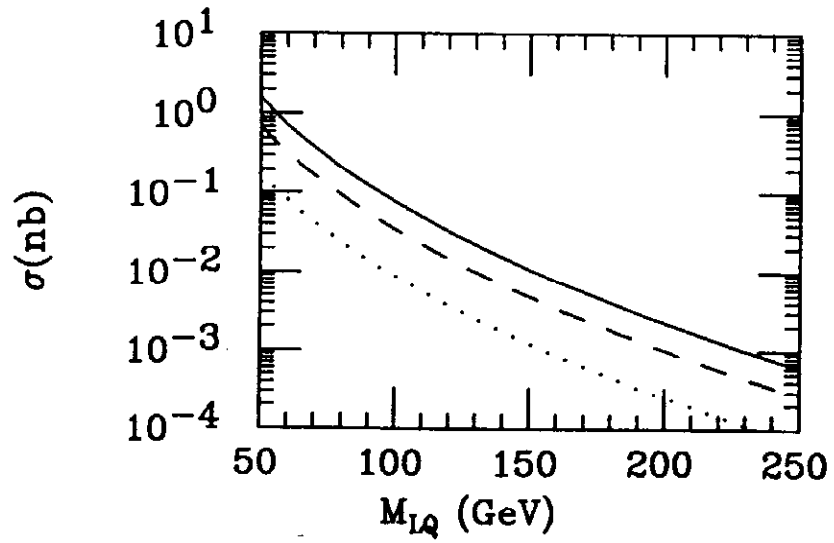


Figure 3b

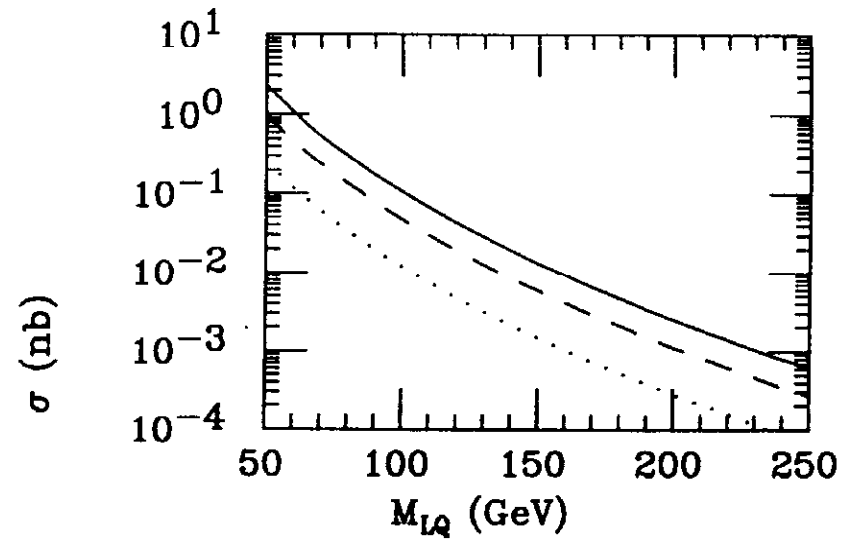


Figure 4a

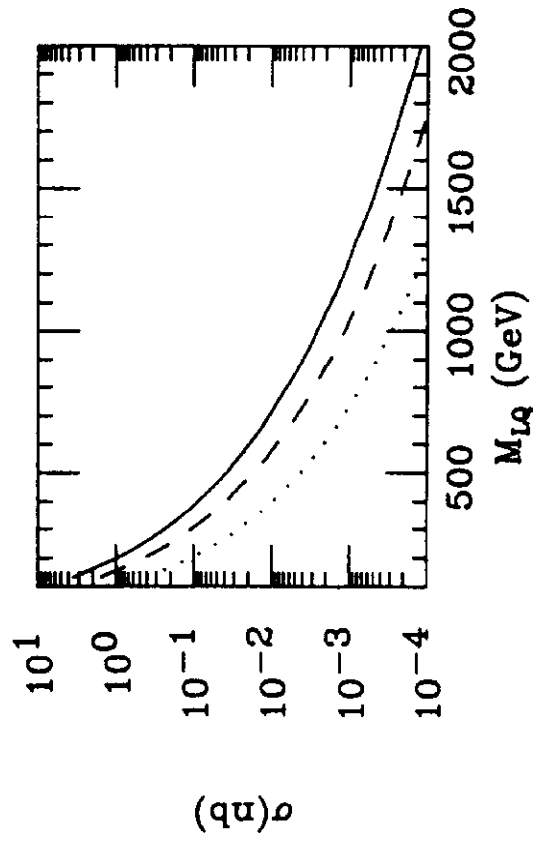
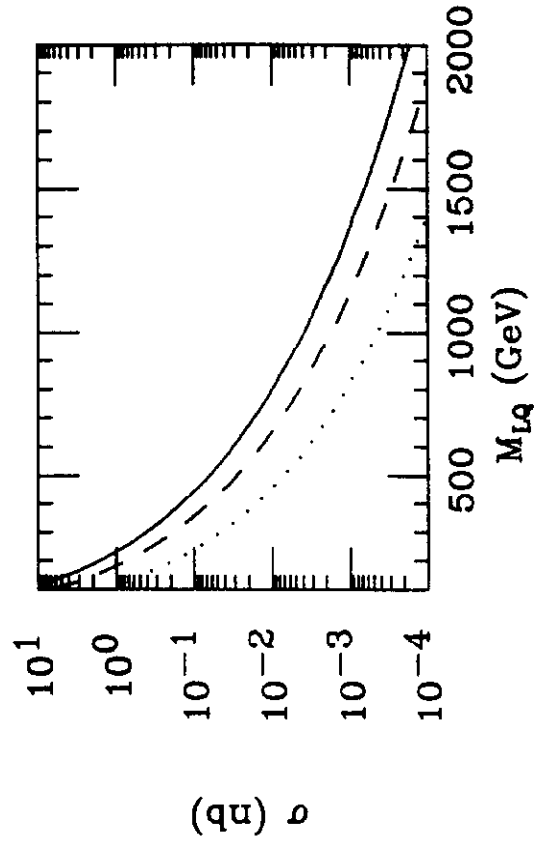


Figure 4b



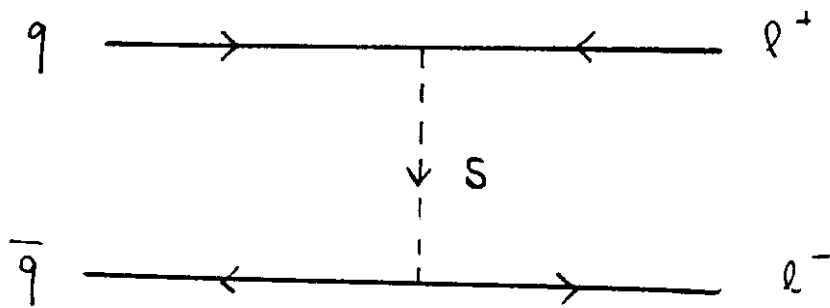
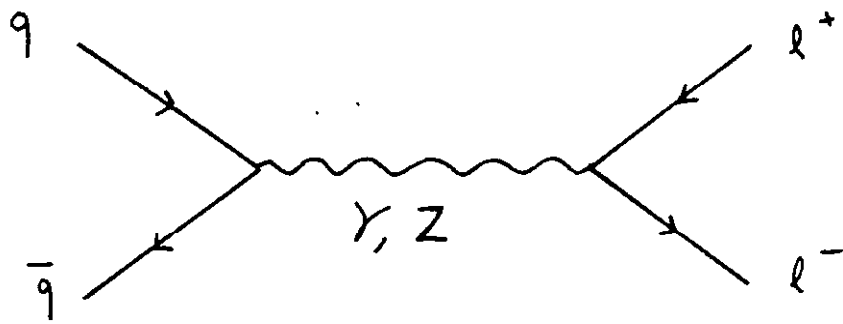


Fig. 5

Figure 6a

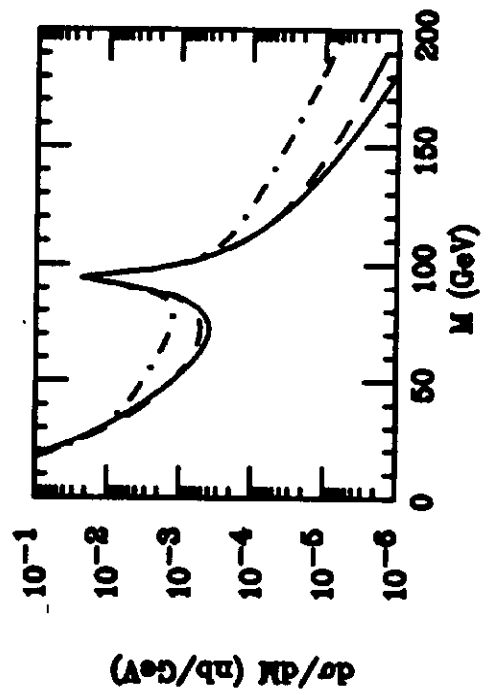
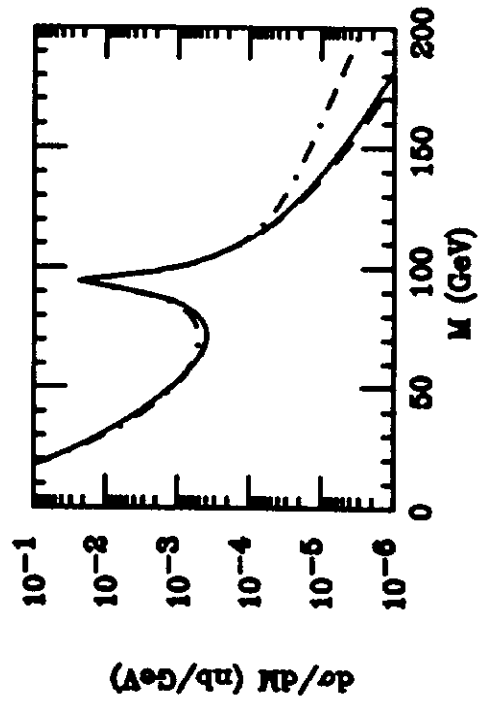


Figure 6b



71

Figure 7a

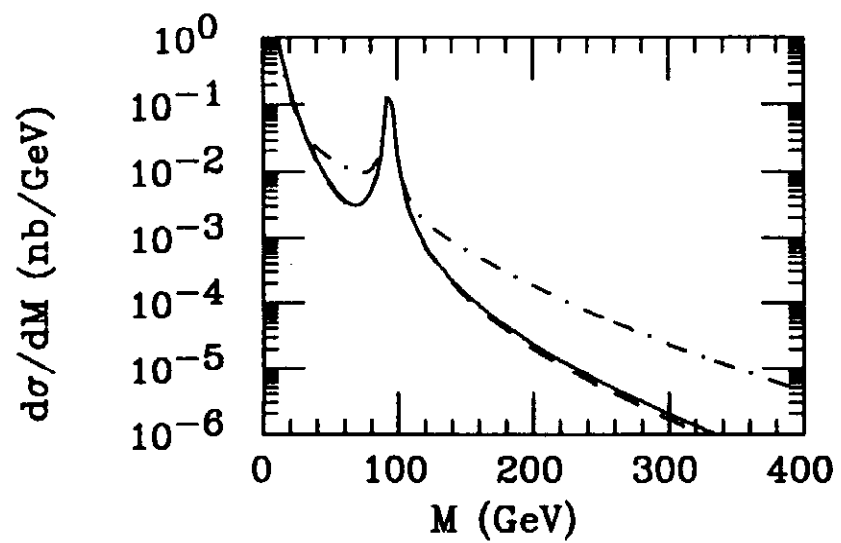


Figure 7b

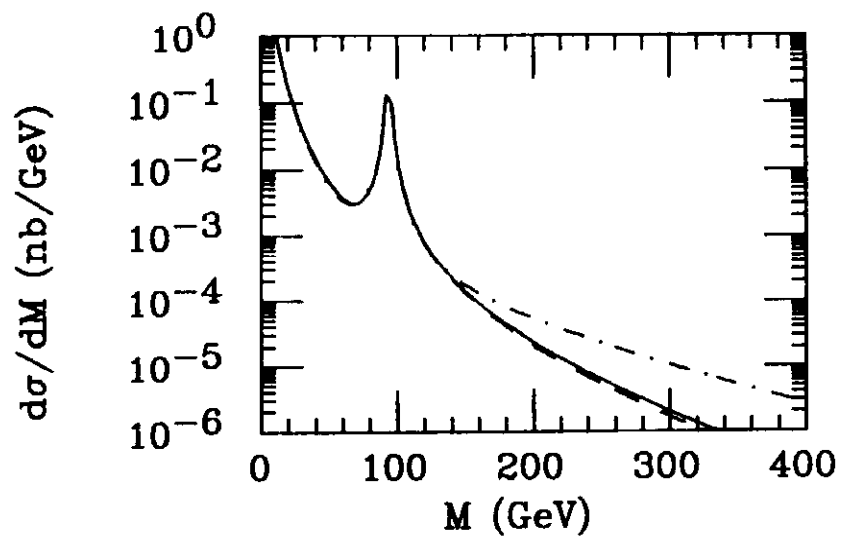


Figure 8a

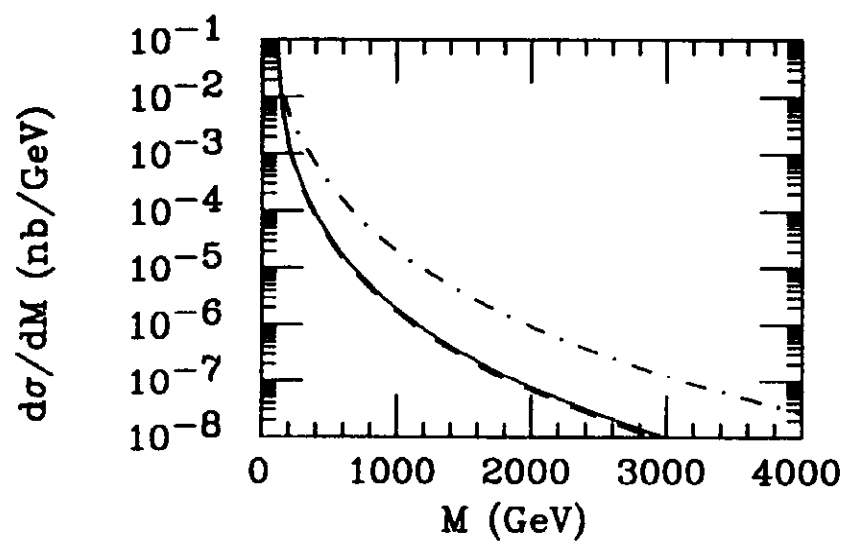
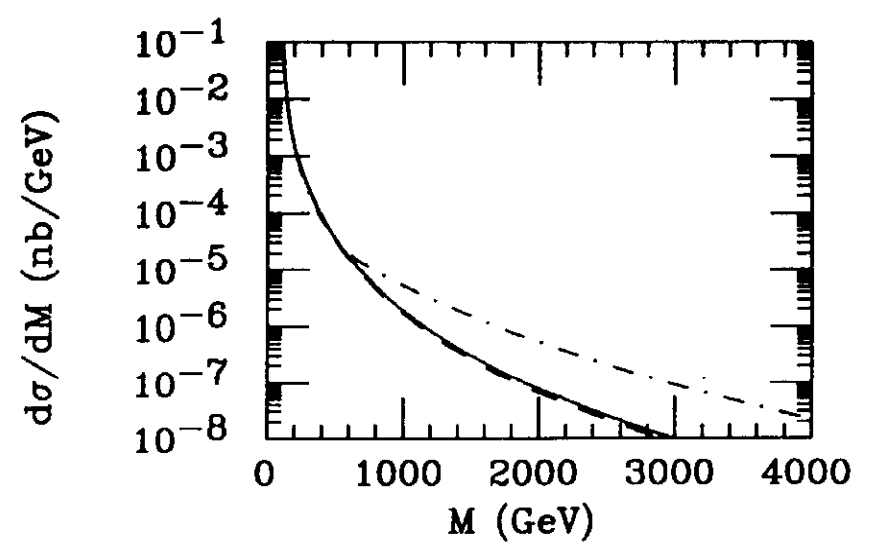


Figure 8b



61

Figure 9

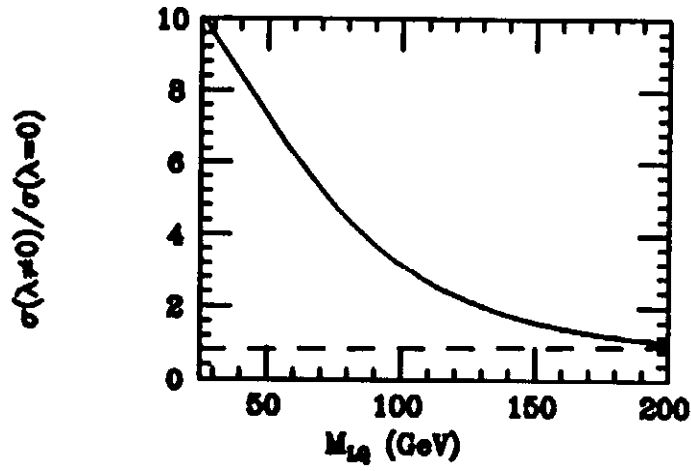


Figure 10

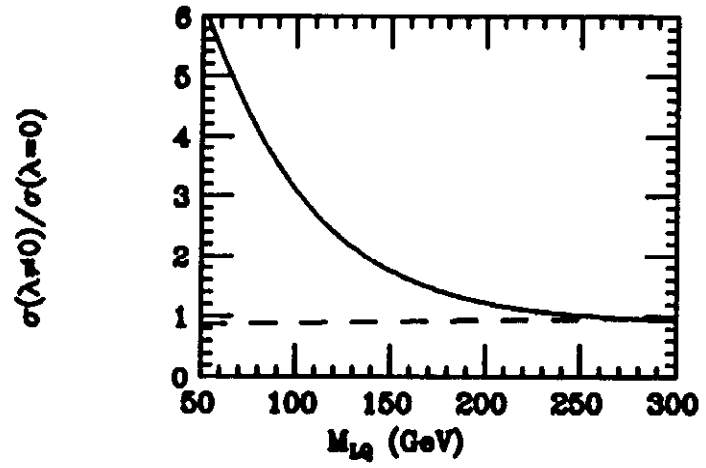


Figure 11

